

# A 26-GHz Miniaturized MIC Transmitter/Receiver

EIJI HAGIHARA, HIROYO OGAWA, NOBUAKI IMAI, AND MASAMI AKAIKE, MEMBER, IEEE

**Abstract**—A very compact 26-GHz transmitter/receiver for high-speed digital radio subscriber systems has been developed. The transmitter/receiver makes extensive use of MIC technology in the RF sections. Transmitting power of 18 dBm and a receiving noise figure of less than 12 dB is obtained. The frequency of the local oscillator is stabilized to within  $\pm 100$  ppm by means of a high-*Q* dielectric resonator. The bit error rate is measured in order to evaluate the overall system, and good performance of the equipment is obtained. A field test using this equipment is now under way. The technique described in the text can be extended to transmitter/receiver for terrestrial radio relay systems and satellite communication systems. In addition, the various MIC components developed here can be scaled to the millimeter-wave region.

## I. INTRODUCTION

**I**N RECENT YEARS, local distribution digital radio systems have been attracting growing interest [1], [2]. In such systems, many subscriber transmitter/receivers are connected to a distribution base station [1], [2]. Cheap, compact transmitter/receivers with high reliability are indispensable for realizing such systems. The microwave integrated circuit (MIC) is considered to be the best method to meet these requirements. Efforts to realize various MIC components and subsystems have been made in the microwave region, and above [3]–[6].

However, to realize a transmitter/receiver for practical application in subscriber equipment, a full-scale integration of the whole RF section of the equipment is desirable.

This paper describes a very compact 26-GHz-band MIC transmitter/receiver intended for use in high-speed digital radio subscriber loop systems [2].

In general, two approaches to building MIC's are possible. 1) An individual circuit component, which usually has one function, is fabricated on a substrate and then the substrates are connected by thin ribbons and/or thin wires. 2) A circuit with two or more functions is made on one substrate.

The choice of approaches depends upon the function of the circuit and the fabrication process (including performance checks). We have adopted the first approach. At present, that approach is considered to be better for lowering equipment cost and obtaining characteristics with little variation, because the fabrication process can be simplified and damaged circuits can easily be replaced.

The main features of the transmitter/receiver are as follows.

- 1) All RF active and passive circuits, except the antenna and transmit/receive branching filter section, are integrated into a compact plane module.
- 2) Low conversion loss performance is obtained from a double-balanced mixer, which uses a combination of various MIC transmission lines on both sides of the dielectric substrate [5].
- 3) Degradation in electrical performance due to undesired coupling between circuits, which is one of the biggest problems with open-boundary circuits, is minimized.
- 4) Stabilization of the local oscillator is realized at 26 GHz by means of a high-*Q* dielectric resonator.

5) An amplitude-shift-keying (ASK) modulator is adopted. A high ON/OFF ratio and low insertion losses are obtained using a three-stage p-i-n diode modulator.

In the following sections, we describe the outline of the equipment, and then describe the design considerations of the various MIC components. Finally, we evaluate the performance of the transmitter/receiver. The main stress is placed on describing the MIC modules of the equipment.

## II. TRANSMITTER/RECEIVER LAYOUT

The construction of the transmitter/receiver is shown in Fig. 1.<sup>1</sup> It is composed of four sections: 1) antenna and transmit/receive filter section; 2) transmitter section; 3) receiver section; 4) modulator/demodulator (MODEM) section. The conceptual outline of this subscriber loop system is shown in the Appendix.

### A. Antenna and Transmit/Receive Filter Section

This section consists of an antenna (ANT), a circulator, and two bandpass filters (T-BPF and R-BPF). ANT is a metal-plated plastic Cassegrain type with a diameter determined by the distance from the subscriber to the base station. For example, an antenna with a radius of 150 mm has an antenna gain of 35 dB, which satisfies system requirements for subscribers within a 3-km radius. The antenna can be adjusted in ranges of  $-10^\circ$ – $+20^\circ$  in elevation and  $\pm 90^\circ$  in azimuth. The calculator routes the

Manuscript received July 15, 1981; revised October 9, 1981.  
The authors are with the Radio Transmission Section, Yokosuka Electrical Communication Laboratory, Nippon Telegraph and Telephone Public Corporation, 1-2356 Take, Yokosuka-shi, 288-03 Japan.

<sup>1</sup>The construction of the base equipment is the same as for the subscriber equipment except for the following points. 1) The AGC circuit is omitted from the base equipment. 2) A limiter circuit is adopted in the base equipment.

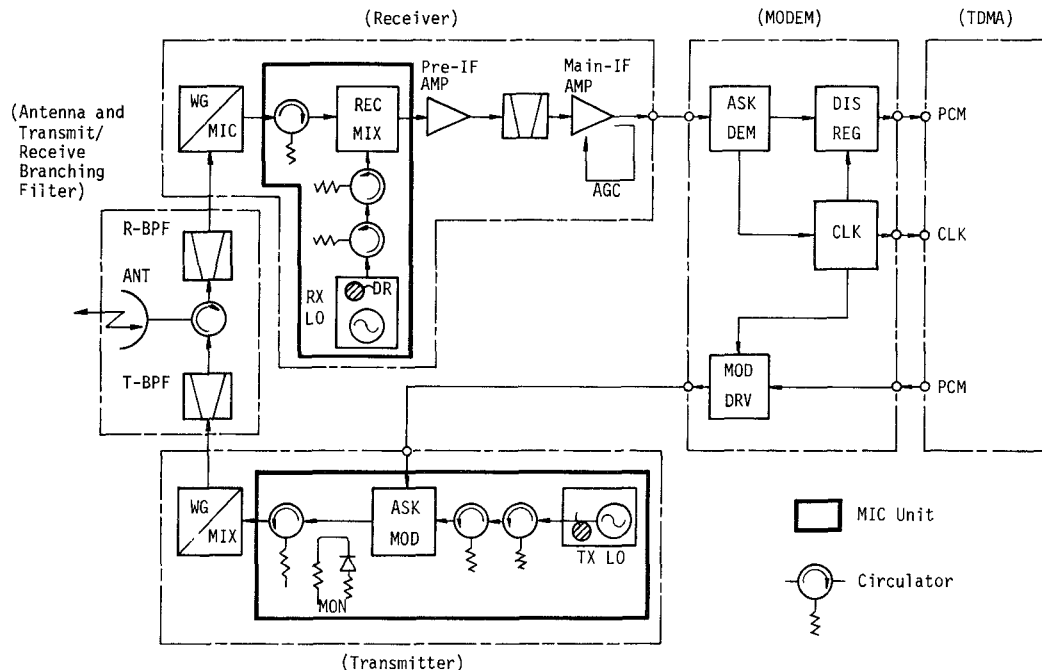


Fig. 1. Block diagram of the subscriber transmitter/receiver.

transmitting and receiving signals. The waveguide BPF's reduce out-band signal spectrum interference and spurious interference.

#### B. Transmitter Section

The transmitter section consists of a local oscillator (TX LO) and ASK modulator (ASK MOD), a transmitting power monitor, circulators, and an MIC-waveguide transition (WG/MIC). All RF circuits (TX LO, ASK MOD, transmitting power monitor, and circulators) are constructed on one plane using MIC technology. In Fig. 1, the thick lines show the integrated RF circuits.

The frequency of the LO is directly modulated by the ASK MOD which is driven by a 15.36-MHz pulse driver (MOD DRV) in the MODEM section. The transmitter signal is fed into the WG/MIC, where the microstrip mode is transformed into the waveguide mode.

#### C. Receiver Section

The receiver section consists of a waveguide-MIC transition (MIC/WG), a receiver mixer (REC MIX), a local oscillator (RX LO), circulators, pre- and main-IF amplifiers, and a bandpass filter (BPF). These circuits are also shown by thick lines in Fig. 1.

The RF signal from the R-BPF is fed into the WG/MIC, and transformed from the waveguide mode into the microstrip mode. The RF signal and the LO output are fed into the REC MIX, where the RF signal is converted into a 140-MHz IF signal. The frequency of the LO is stabilized by a dielectric resonator. The IF signal is amplified by the pre- and main-amplifiers. Undesired noise outside the signal band is eliminated by the bandpass filter. The IF output power level is kept constant using AGC from the main IF amplifier.

#### D. MODEM Section

This section mainly consists of an ASK detector (ASK DET), a decision and regenerating circuit (DES REG), a timing recovery circuit (CLK), and a pulse driving circuit (MOD DRV).

In the ASK DET, envelope detection from IF into a baseband signal is performed, and the clock signal is extracted. The detected signal is fed into the DES REG. Regenerated pulses and the clock signal are sent to the TDMA section. The MOD DRV, which is driven by a signal from the TDMA section, drives the ASK MOD for the transmitter.

### III. MIC COMPONENTS

#### A. IMPATT and Gunn Local Oscillators

To realize a compact and low-cost transmitter/receiver, it is indispensable to integrate local oscillators by MIC technology.

For this purpose, an IMPATT diode is used in the transmitter local oscillator to obtain high transmitting power, and a Gunn diode is used in the receiver to improve the noise figure. A band-rejection-type oscillator stabilized by a  $TE_{018}$ -mode dielectric resonator has been employed due to the simplicity of the fabrication process and the compactness of the circuit.

1) *Equivalent Circuit and Stable Oscillation:* An oscillator circuit with a microstrip line is schematically shown in Fig. 2. The circuit consists of an encapsulated IMPATT diode, a microstrip line, a dielectric resonator, a dc bias circuit, a dc block, and a load. An equivalent circuit corresponding to Fig. 2 is shown in Fig. 3. In the figure,  $Z_d(v)$  is the active impedance of the IMPATT diode and is assumed approximately to be a function of applied RF

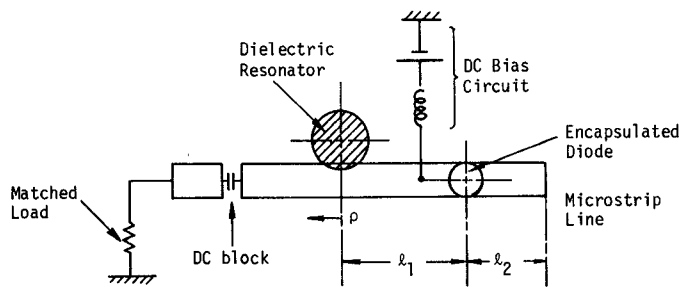


Fig. 2. Schematic structure of the stabilized IMPATT oscillator.

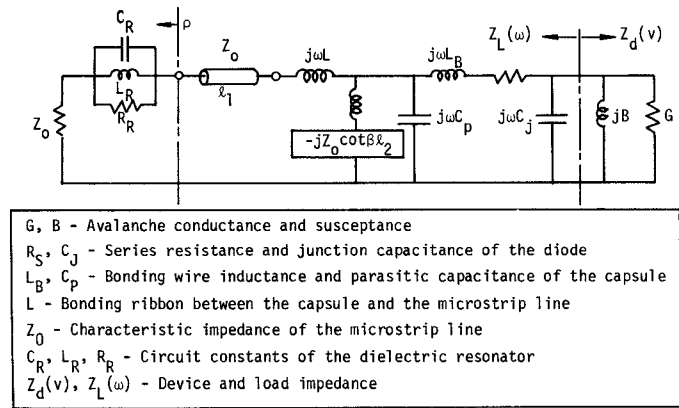
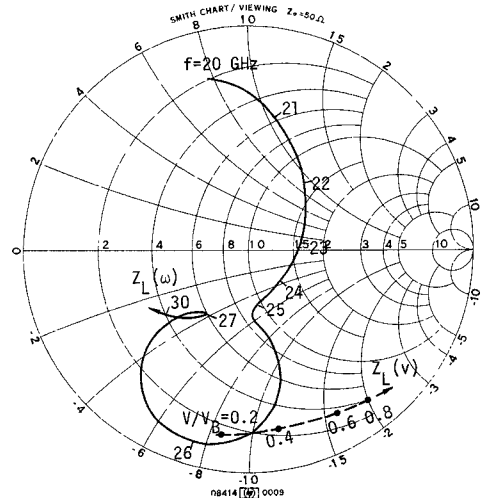


Fig. 3. The equivalent circuit of the stable IMPATT oscillator.

Fig. 4. The relationship between the device line and the load line of the stabilized IMPATT oscillator. The solid line corresponds to the load line, and the dotted line to the device line. The resonant frequency of the dielectric resonator  $f_0$  is 26 GHz,  $\rho = 10$ ,  $Z_0 = 25$ ,  $l_1 = 4.35$  mm, and  $l_2 = 1.6$  mm.

voltage on the junction  $Z_d = G + jB$ . On the other hand  $Z_L(\omega)$  is the load impedance and is a function of frequency (containing the passive impedance of the diode,  $C_j$ ,  $C_p$ ,  $L_p$ ,  $R_s$ ).

In order to obtain a stable oscillator condition,  $Z_d(v)$  and  $Z_L(\omega)$  have been plotted on a Smith chart, as functions of  $v$  and  $\omega$ , respectively. The active impedance  $Z_d(v)$ , are obtained according to the computer analysis developed by Shindo and Okamura [7]. The relationship between  $-Z_d(v)$  and  $Z_L(\omega)$  are shown in Fig. 4. Circuit param-

ters,  $l_1$ ,  $l_2$ ,  $Z_0$ , and  $\sigma$  in the load impedance are decided so that the load line and device line in the Smith chart satisfies Kurokawa's criteria [8]. The cross point of both lines corresponds to the load impedance where a stable oscillation is obtained. In this case, the oscillation frequency of 25.98 GHz and the oscillation power of 1.5 W (in real case, the oscillation power is reduced by the circuit loss due to  $R_s$ ,  $C_j$ , etc.) are expected ( $l_1 \simeq 2\lambda_g/4$ ,  $l_2 \simeq \lambda_g/4$ ,  $Z_0 = 25 \Omega$ ,  $\rho = 10$ ).

2) *Stabilization of the Oscillation Frequency*: The temperature coefficient of the oscillation frequency  $\Delta f_o/\Delta T$ , can be expressed as [3]

$$\frac{\Delta f_o}{\Delta T} = \tau_{DR} - \frac{F(\rho)}{Q_0} \cdot \frac{\Delta X_d}{\Delta T}, \quad F(\rho) = \frac{\rho^2}{2(\rho-1)} \quad (1)$$

where the first term corresponds to the temperature coefficient of the dielectric resonator  $\tau_{DR}$ , and the second term to the temperature coefficient of the diode reactance,  $\Delta X_d/\Delta T$ .  $F(\rho)$  is a function of the VSWR  $\rho$  seen toward the load at the plane of the resonator, and has the minimum value when  $\rho = 2$  (since  $\rho \geq 1$ ).  $Q_0$  is the unloaded  $Q$  factor of the resonator.

In order to minimize the frequency deviation of the oscillator, the dielectric resonator should be chosen according to the following methods: 1) to use a dielectric resonator with a high  $Q_0$  value, in order to suppress the frequency deviation of the diode reactance in the first term; 2) to use a dielectric resonator with a positive  $\tau_{DR}$  value, in order to cancel the first term (which is usually a negative value), if  $Q_0$  does not completely suppress the frequency deviation of the diode reactance.

For this purpose, a chemical compound of (ArSn)  $TiO_4$  [9] ( $\epsilon_r = 37$ ) was employed as a dielectric resonator. The resonant frequency and the unloaded  $Q$  factor of the dielectric resonator were adjusted by a metal housing surrounding the dielectric resonator [10]. The value of  $Q_0$  and  $\tau_{DR}$  of the dielectric resonator used here was 2000 and 4 ppm at 26 GHz.

3) *Oscillation Characteristics*: Free running oscillation characteristics of the diode chip were measured to check the tunability. The diode used here is a silicon DDR diode with a diamond heatsink, which typically has a breakdown voltage  $V_B$  of 44 V, and a junction diameter  $d$  of 80  $\mu m$ . The relationship between the oscillation power and frequency is shown in Fig. 5. In the experiment, load impedance are optimized at each point. It is seen that the maximum oscillation power is obtained around 27 GHz.

Fig. 6 shows oscillation characteristics of the stabilized oscillator using an encapsulated diode as a function of ambient temperature. The diode is mounted on the circuit described in Fig. 2. In the circuit, an MIC circulator is used to provide isolation between the diode and the load. The oscillation power of 26 dBm is obtained at 26.28 GHz. The junction temperature rise is estimated to be less than 180°C which corresponds to a failure rate of 2300 bits. [11]. The output power deviation is less than  $\pm 1$  dB for the temperature range  $-5^\circ C$  to  $+50^\circ C$ . The frequency deviation is less than 2 MHz in the same temperature range.

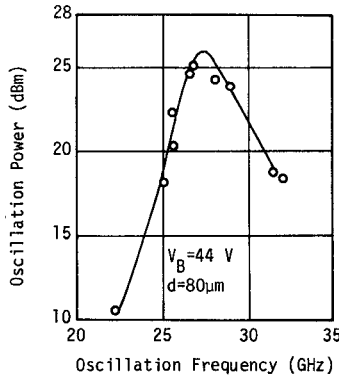


Fig. 5. Oscillation characteristics of the chip-type IMPATT diode.

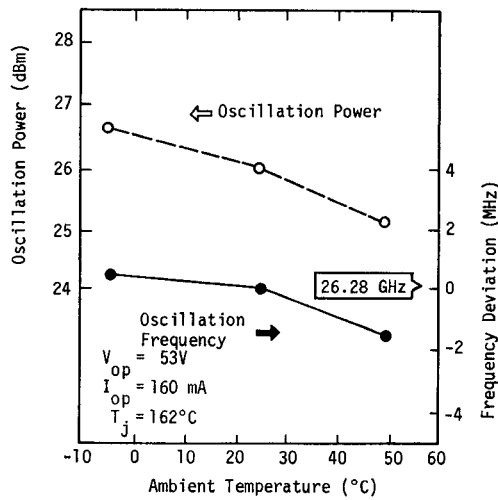


Fig. 6. Temperature dependence of the power and frequency of an MIC IMPATT local oscillator. The frequency is stabilized by a dielectric resonator.

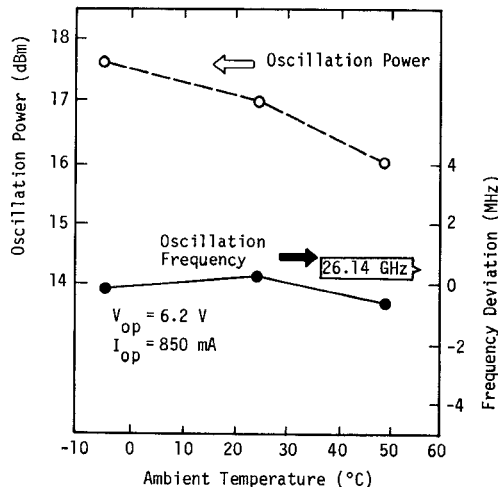
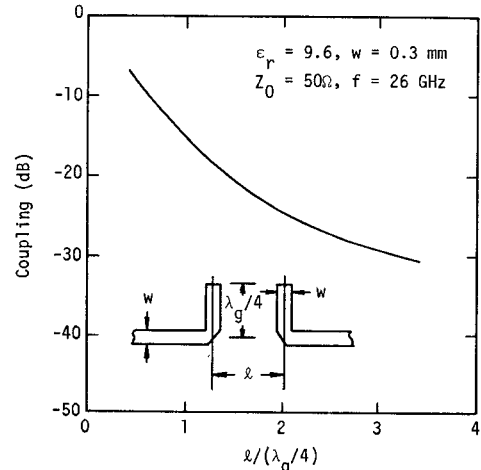


Fig. 7. Temperature dependence of the power and frequency of an MIC Gunn local oscillator. The frequency is stabilized by a dielectric resonator.

The Gunn oscillator was obtained based on the same consideration. Fig. 7 shows the oscillation characteristics as a function of ambient temperature. The stabilized oscillation power is 16 dBm at 25°C, which is enough power to derive the receiver mixer. The output power deviation is

Fig. 8. Coupling between two separated  $\lambda_g/4$  stubs as a function of spacing  $l$ .

less than  $\pm 1$  dB and the frequency deviation is less than 2 MHz at 26.14 GHz for the temperature range  $-5^\circ\text{C}$  to  $+50^\circ\text{C}$ .

#### B. ASK Modulator

In the radio subscriber loop system, the ASK modulator in a subscriber transmitter is required to have a high ON/OFF ratio to prevent the burst-signal emitted from one subscriber from being interfered with by the leaked power of other subscribers [2]. The modulator in this system is required to have an ON/OFF ratio of 60 dB.

To obtain a high ON/OFF ratio, a multistage modulator is required. However, if there is some unwanted coupling between modulator diode connection lines, the upper limit of the ON/OFF ratio may be restricted.

In this section, we will first estimate the amount of unwanted coupling. Then we will describe the structure and characteristics of a high ON/OFF-ratio ASK modulator.

1) *Unwanted Coupling*: We estimated the amount of coupling between two separated transmission lines using the model shown in Fig. 8, where two  $\lambda_g/4$  stubs are faced in parallel. In the figure, the coupling between the two stubs is shown as a function of spacing  $l$ . The unwanted coupling is considered to be due to the radiation of power from the stub into the open air. From the figure, it is shown that coupling in the order of 40 dB is inevitable if no scheme for suppression of radiation is used.

2) *High ON/OFF-Ratio ASK Modulator*: To reduce coupling, we have made use of a conductive cutoff rectangular-waveguide housing. It is designed to reduce coupling through the open air. The width of the housing was selected so that the  $\text{TE}_{10}$ -mode cutoff attenuation would exceed 60 dB/ $\lambda$  at 26 GHz, as shown in Fig. 9. The three diodes are covered by the cutoff waveguide. They are cascade connected with gold wires. The circuit consists of three chip-type p-i-n diodes, a thin gold bonding-wire, the conductive cutoff rectangular-waveguide housing described above, and two microstrip lines.

An ON/OFF ratio of over 60 dB has been realized, with

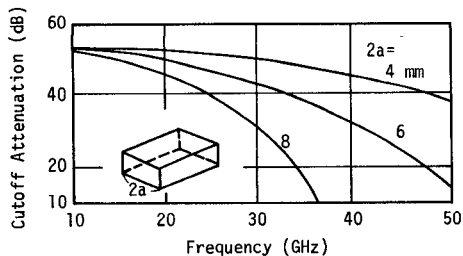


Fig. 9. Cutoff attenuation of a rectangular waveguide as a function of frequency.

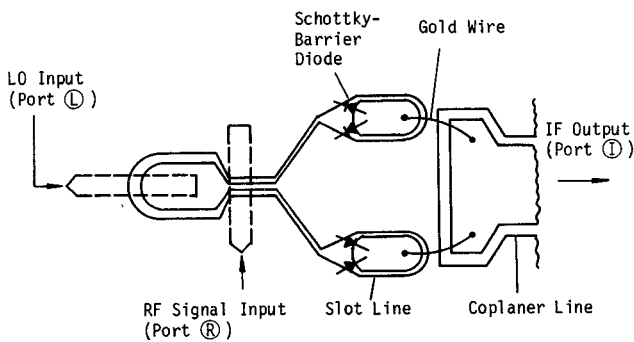


Fig. 10. Schematic of the double-balanced-type receiving mixer.

the housing, in the 24–28-GHz range. The insertion loss of less than 1.5 dB and a VSWR of less than 2 has been realized in the above frequency range. The rise and fall times of the modulator output waveform are in order of 5 ns.

### C. Receiving Mixer

The double-balanced-type mixer used in the receiver is schematically shown in Fig. 10. This mixer uses a combination of microstrip lines, a slot line, and a coplanar line, which are made on both sides of the substrate. The dotted lines correspond to the microstrip lines and the solid lines correspond to the slot line and the coplanar line. The slot line is connected to the coplanar line by gold wires.

The diodes used here are GaAs Schottky-barrier mixer diodes, which typically have a series resistance of  $0.45\ \Omega$ , a zero-bias junction capacitance of  $0.12\ \text{pF}$ , and a breakdown voltage of 8 V.

In the figure, the RF signal and LO output are fed into an MIC magic-T through two microstrip lines. (Port ② and port ① in the figure, respectively.)

They are split into two parts and fed in two two pairs of diodes through two slot lines. The pair of diodes connected to one slot loop are excited in-phase by the RF signal, but out-of-phase by the LO output. The pair of diodes connected to the other slot loop are excited in-phase by both the RF signal and the LO output. Therefore, both the RF signal and the LO output are cancelled, and only the IF signal is obtained, through the two gold wires.

This type of mixer has the following advantages: 1) undesired waves, such as the LO output and any image signals, are eliminated without filters; 2) the circuit for the IF port is easily fabricated using thin Au wires; 3) good performance can be obtained in a higher frequency region.

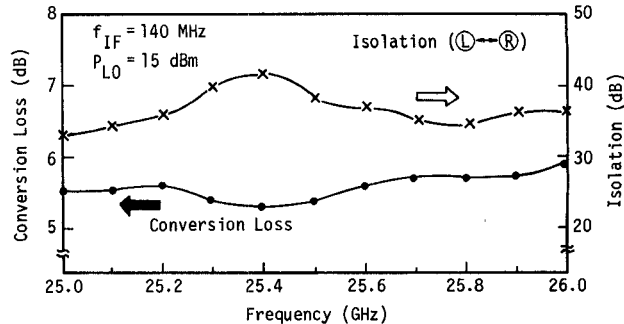


Fig. 11. Conversion loss and isolation in the receiving mixer as a function of frequency.

Experimental results for the mixer are shown in Fig. 11. The conversion loss from port ② to port ① is measured in the RF frequency range 25.0–26.0 GHz with a LO output  $P_{LO}$  of 15 dBm and a fixed IF frequency  $f_{IF}$  of 140 MHz. The frequency response of the conversion loss is very flat, less than 6 dB across the whole range. The minimum value is obtained at 25.3 GHz. The isolation between port ② and port ① was measured under the same conditions as for the measurement of conversion loss. Isolation greater than 30 dB over the entire range was obtained. It should be noted that the maximum value was obtained at 25.4 GHz, which corresponds to the minimum point of the conversion loss.

### IV. TRANSMITTER/RECEIVER MODULE EVALUATION

The MIC components described in detail in the previous sections have been arranged and composed into a compact transmitter/receiver module.

Fig. 12 shows an internal view of that module. Each MIC component is fixed to a metal carrier by conducting epoxy resin and connected by gold ribbon using thermal bonding. The net areas for the MIC module are  $1.7\ \text{cm} \times 1.7\ \text{cm}$  for the transmitter and  $2.1\ \text{cm} \times 2.1\ \text{cm}$  for the receiver. Thus, a very compact transmitter/receiver module has been realized for the 26-GHz band.

Major characteristics of the transmitter/receiver are shown in Table I. The transmitter output power is 18 dBm at 26 GHz. The frequency stability of the transmitter is better than  $\pm 100\ \text{ppm}$  in the  $-5^\circ\text{C}$  to  $+50^\circ\text{C}$  range. The receiving noise figure is less than 12 dB.

The circuit loss from the local oscillator to the transmitter output is 8 dB. Table II shows the loss for each MIC component. Losses due to substrate connection are estimated to be 0.3 dB/connection. To improve the output power, reduction of connection losses is required.<sup>2</sup>

The external view of a subscriber radio unit is shown in Fig. 13. A Cassegrain type antenna with a radius of 150 mm can be seen at the top of the equipment.

<sup>2</sup>The value of 0.3 dB/connection is somewhat large. In this case conducting epoxy resin has been used. It is considered that the loss is mainly due to imperfection of electrical contact at the ground conductor junction of the substrate.

TABLE I  
CHARACTERISTICS OF THE MIC TRANSMITTER AND  
RECEIVER

SECTION	MAIN COMPONENT	ITEM	CHARACTERISTICS
Antenna & Transmit/Receive Branching Filter	Antenna	Gain (Diameter)	35 dB (30 mm)
	Circulator (WG Type)	Isolation Insertion Loss	20 dB 0.2 dB
	Transmit Bandpass Filter (3rd Order Maximal Amplitude Flat Type)	3-dB Band Width	±25 MHz
	Receive Bandpass Filter (3rd Order Maximal Amplitude Flat Type)	3-dB Band Width	±50 MHz
Transmitter	Local Oscillator (IMPATT)	Output Power Frequency Stability	26 dBm within ±100 ppm (-5 ~ 50°C)
	ASK Modulator (PIN)	ON/OFF Ratio Insertion Loss	more than 60 dB 1 dB
Receiver	Local Oscillator (Gunn)	Output Power Frequency Stability	17 dBm within ±100 ppm (-5 ~ 50°C)
	Receiving Mixer (Schottky)	Conversion Loss	6 dB
	Pre-IF Amplifier	Noise Figure Gain	1.5 dB 30 dB
	Main IF Amplifier	Gain AGC Range	70 dB more than 45 dB
	IF Bandpass Filter (2nd Order Maximal Amplitude Flat Type)	3-dB Band Width	15 MHz
MODEM	Timing Recovery Circuit	Phase Error Locking Range	less than 10° less than 1 kHz
Common	Circulator (MIC Type)	Isolation Insertion Loss	20 dB 0.8 dB
	WG/MIC	VSWR Insertion Loss	1.2 dB 0.3 dB
Transmitting Power			18 dBm
Receiving Noise Figure			10 dB
Net Frequency Stability			within ±100 ppm (-5 ~ 50°C)

TABLE II  
INSERTION LOSSES IN TRANSMITTER COMPONENTS

SECTIONS	COMPONENTS	LOSS (dB)
MIC SECTION	ASK MOD	1.0
	CIR (2 pieces)	1.6 (= 0.8 × 2)
	MON	0.3
	WG/MIC	0.3
WAVEGUIDE SECTION	BPF	2.2
	CIR	0.2
TOTAL LOSS		5.6
CONNECTION LOSS		0.3/CONN.

Behind the antenna, two bandpass filters and the circulator for the antenna and transmit/receive filter section, transmitter section, and receiver section are housed inside a plastic box and joined to the antenna. The temperature in the box is less than 50°C, which ensures the reliability of

the transmitter/receiver. The IF and baseband circuits and stabilized power supplies are housed in a plastic box under the antenna and transmitter/receiver module. Total dissipation power of the equipment is 50 W, which is provided from a commercial ac 100-V power source.

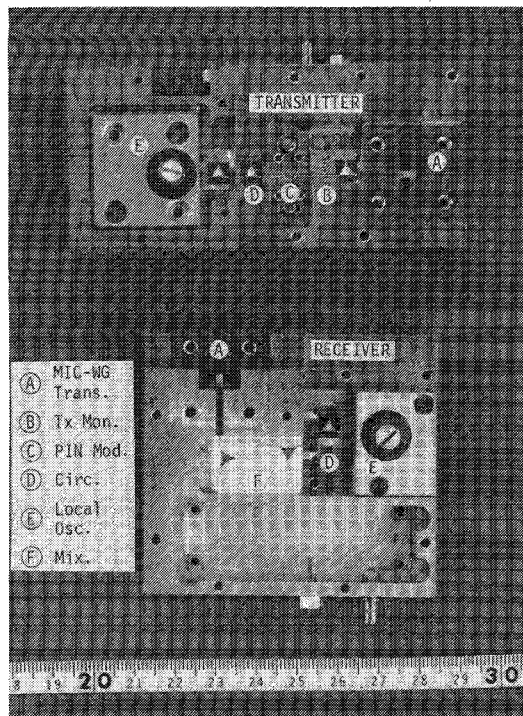


Fig. 12. Internal view of the transmitter and receiver sections. The empty space in the receiver is for the pre-IF amplifier.

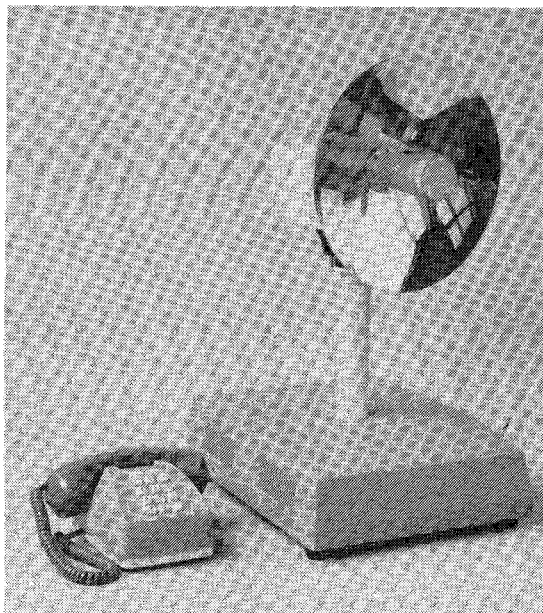


Fig. 13. External view of the transmitter/receiver equipment of a subscriber.

This equipment is very compact (as can be seen in the picture) and portable (the total weight is about 15 kg), and is designed to be adaptable to the atmosphere inside offices.

Overall system evaluation was performed by measuring the bit error rate between a base and subscriber equipment.

The bit error rate for the path from the base to the subscriber was measured in a 15.36-MHz pseudorandom pulse mode. The results are shown in Fig. 14. Deterioration

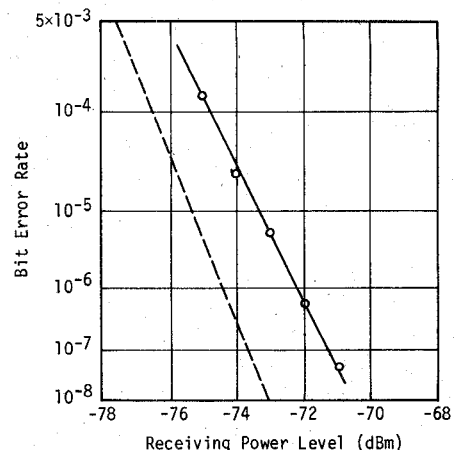


Fig. 14. System bit error rate as a function of receiving power level. Dotted line shows ideal theoretical values and circles show the experimental values.

from the ideal theoretical value is 2 dB at a  $10^{-4}$  error rate. A field test using this equipment is now under way.

## V. CONCLUSIONS

A very compact 26-GHz transmitter/receiver for high-speed digital radio subscriber systems have been developed. The transmitter receiver makes extensive use of MIC technology in the RF sections.

Transmitting power of 18 dBm and a receiving noise figure of less than 12 dB have been obtained. A frequency deviation of less than  $\pm 100$  ppm has been realized by means of a high-*Q* dielectric resonator. The bit error rate has been measured between the base station and the subscriber in order to evaluate the overall system, and the equipment performed well.

A field test is now under way using the base station equipment and the subscriber equipment described in the text.

The technique described here can be extended to transmitter/receivers for terrestrial radio relay systems and satellite communication systems.

In addition, the various MIC components developed here can be scaled to beyond the 30-GHz region.

## APPENDIX

Fig. 15 shows a conceptual view of the radio subscriber loop system. The network consists of base stations (local offices at the telephone service hierarchy) and subscribers which are connected to the nearest base station.

A base station provides service to several tens of subscribers within a radius of about 7 km.

Transmission from a base station to subscribers is performed in the time division multiplex (TDM) mode. Each subscriber accepts and decodes only the transmission bursts which are addressed to him.

On the other hand, transmission from subscribers to a base station is performed in the time division multiple access (TDMA) mode. Subscribers transmit data through assigned time slots.

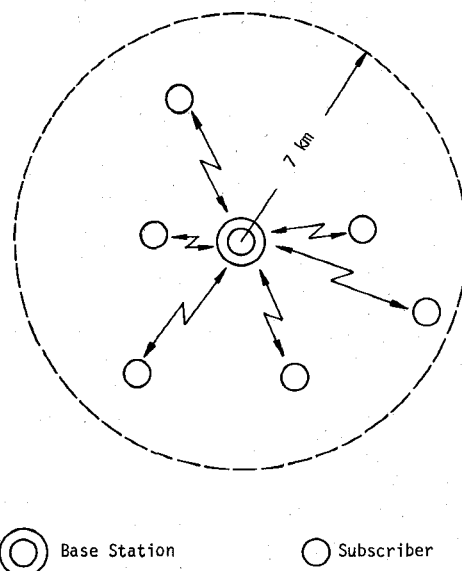


Fig. 15. Conceptual view of the radio subscriber loop system. Each subscriber is connected to the nearest base station. The service area is within 7 km.

Differences in receiving power levels from the base station to subscribers at various distances are compensated by changing the subscriber antenna diameter, so that system reliability is kept within a certain value. Differences in propagation delay time are adjusted by subscribers, so that all subscriber bursts are aligned when they arrive at the base station.

#### ACKNOWLEDGMENT

The authors wish to thank Dr. Yamamoto for his continuous encouragement and guidance, and Dr. Kurita, Dr. Shindo, and Dr. Aikawa for their fruitful discussions. The authors also wish to express their thanks to the members of Fujitsu Laboratories, Ltd., for their cooperation in equipment manufacturing.

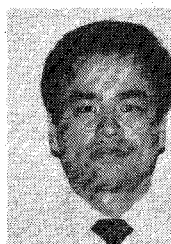
#### REFERENCES

- [1] J. Fawcette, "Local radios grafted to SBS net," *MSN*, pp. 21-25, June 1980.
- [2] S. Shindo, O. Kurita, and M. Aikawa, "Radio subscriber loop system for high-speed digital communications," *ICC Dig.*, vol. 66.1, 1981.
- [3] T. Makino and A. Hashima, "A highly stabilized MIC Gunn oscillator using a dielectric resonator," *IEEE Trans. Microwave Theory Tech.*, vol. MTT-27, pp. 633-638, July 1979.
- [4] M. Aikawa and H. Ogawa, "2 Gb double-balanced PSK modulator using coplanar waveguides," *BSSC Dig. Tech. Pap.*, Feb. 1979, pp. 172-173.
- [5] H. Ogawa, M. Aikawa, and K. Morita, "K-band integrated double-balanced mixer," *IEEE Trans. Microwave Theory Tech.*, vol. MTT-28, Mar. 1980, pp. 180-85.
- [6] M. Hata, A. Fukasawa, M. Bessho, S. Makino, and H. Higuchi, "A 40-GHz digital distribution radio with a single oscillator," *IEEE Trans. Microwave Theory Tech.*, vol. MTT-28, pp. 951-962, Sept. 1980.
- [7] Y. Shindo and S. Okamura, "Effect of the circuit of second-harmonic frequency on IMPATT oscillators," *vol. J63-B*, No. 4, 1980, pp. 286-293.
- [8] K. Kurokawa, "Some basic characteristics of broadband negative resistance oscillator circuits," *Bell Syst. Tech. J.*, July-August, vol. 48, No. 6, 1969, pp. 1937-1955.
- [9] H. Tamura, K. Nishida, and K. Wakino, "High permittivity ceramic dielectrics for microwave resonators," *Tech. Group CPM 78-50, IECE Jap.*, pp. 31-38, 1978.
- [10] E. Hagihara, M. Aikawa, and N. Imai, "Radiation suppressed high-Q dielectric resonators for MIC applications," *Electron. Lett.*, vol. 17, pp. 313-314, Mar. 1981.
- [11] K. Fukuta and K. Chino, "Reliability of semiconductor devices for 20 GHz digital radio-relay systems," *ECL Monthly J.*, vol. 24, no. 10, pp. 2311-2325, 1975.

Eiji Hagihara was born in Yokkaichi, Japan, in 1950. He received the B.S. and M.S. degrees in applied physics from Nagoya University, Nagoya, Japan, in 1973 and 1975, respectively.

He joined Yokosuka Electrical Communication Laboratories, Japan, in 1975, and has been engaged in the research of millimeter-wave solid state circuits and millimeter-wave integrated circuits. He is now the manager in Kinki Telecommunication Bureau, N.T.T., Osaka, Japan.

Mr. Hagihara is the member of the Institute of Electronics and Communications Engineers of Japan.

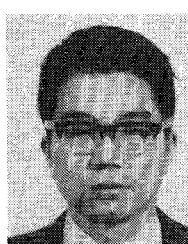


Hiroyo Ogawa, for a photograph and biography please see page 234 of this issue.

Nobuaki Imai was born in Kochi, Japan, in 1953. He received the B.S. degree in electrical engineering from Nagoya Institute of Technology, Nagoya, Japan, in 1975, and the M.S. degree from Kyoto University, Kyoto, Japan, in 1977.

He joined Yokosuka Electrical Communication Laboratories, Japan, in 1977, and has been engaged in the research of millimeter-wave integrated circuits.

Mr. Imai is a member of the Institute of Electronics and Communication Engineers of



Japan.

Masami Aikawa (S'65-M'76), for a photograph and biography please see page 234 of this issue.